Contribution from the Department of Physical and Inorganic Chemistry, University of Adelaide, Adelaide, South Australia, 5001, Australia

Structure, Conformational Analysis, and Optical Activity of a Bis(tridentate)cobalt(III) Complex. $(+)_{589}$-ΔλλBis[1,1,1-tris(aminomethyl)ethane]cobalt(III) Chloride $(+)_{589}$-(*R*,*R*)-Tartrate Hydrate

RODNEY J. GEUE and MICHAEL R. SNOW*

Received July 2, 1976 AIC60478L

The crystal structure of $[(+)_{589}$-Δλλ-$[Co(tame)_2]Cl][(+)_{589}$-*R*,*R*-tart]·$xH_2O$ (tame is $CH_3C(CH_2NH_2)_3$) has been determined from 2692 reflections collected by counter methods. The crystals are monoclinic, space group $P2_1$, with a = 14.631 (3) Å, b = 16.890 (3) Å, c = 8.720 (2) Å, and β = 143.9 (1)°. The measured density is 1.50 (1) g cm^{-3} which agrees with the calculated value of 1.505 for Z = 2. Refinement by blocked full-matrix least-squares gave a conventional R value of 0.025. In solution the $[Co(tame)_2]^{3+}$ cation can have interconvertible meso and racemic conformations. Strain energy minimization calculations show the racemic modification to be 1.6 kcal mol^{-1} more stable than the meso form. The racemic conformer is resolved in the solid state by crystallization as the chloro $(+)_{589}$-tartrate salt, but it rapidly isomerizes on redissolution. The optically active complex cation in the crystal has approximate D_3 symmetry. The conformation of the six-membered chelate rings formed by both of the tridentate chelate caps is λ and the absolute configuration of the complex is designated $(+)_{589}$-Δλλ. The chelate rings have an asymmetric skew-boat conformation. The CoN_6 coordination sphere deviates significantly from O_h symmetry and shows a trigonal-twist distortion of 4.2° from 60° with a small polar elongation along the pseudo-threefold axis of the complex. The hydrogen atoms of the methyl groups were found to adopt staggered positions with respect to the opposing C–C bonds of the quaternary carbon atoms. The cation, two water molecules, and the tartrate ion form an intricate planar network in which the molecular subunits are connected by apparent hydrogen bonds. Other close contacts involving the chloride ion and the remaining water molecules are indicative of weak hydrogen bonding between molecular planes. The geometry of this conformation obtained by strain energy minimization agrees well with the x-ray results. In the solid state the complex has a substantial positive circular dichroism in the region of the $^1A_{1g} \rightarrow {}^1T_{1g}$ transition and in solution it exhibits a Pfeiffer effect with $(+)_{589}$-tartrate ion. These results have been used to evaluate two theories of optical activity. They provide a verification of the crystal field static coupling model of Piper and Karipides for the $Co^{III}N_6$ core and qualitatively confirm the more elaborate model of Richardson which applies to the whole complex.

Introduction

Cobalt(III)–amine complexes with D_3 symmetry have been very important model systems for both theoretical and experimental investigations of optical activity.[1-19] More recent theories of the origin of the circular dichroism (CD) of these complexes have explicitly stated the relationship between stereochemistry and the net rotatory strength of the long-wavelength $^1A_{1g} \rightarrow {}^1T_{1g}$ transition.[3-5,16-19] The known D_3 cobalt(III) complexes of saturated ligands, whose structure and absolute configuration are known, are all tris(bidentate). It was desirable to further evaluate these theories by studying complexes of the same theoretically amenable symmetry but with a widely different disposition of the nonligating ligand atoms. The $[bis(tame)Co^{III}]^{3+}$ complex (tame is 1,1,1-tris(aminomethyl)ethane) has its nonligating atoms above and below the trigonal planes of the donor nitrogens, whereas the tris(bidentate) complexes such as $[Co(en)_3]^{3+}$ (en is ethylenediamine) have theirs between the opposed trigonal planes. The three possible conformational isomers of the $[Co(tame)_2]^{3+}$ ion can be designated λλ, δδ, and λδ or δλ where δ and λ refer[20] to the conformations of the skew-boat rings of the Co–tame moiety. The first two conformers are optical isomers and the second two are identical meso isomers. The minimum stain energy form of the δδ (or λλ) isomer has symmetry D_3 and the δλ (or λδ) form, C_{3i}. The isomers are shown in Figure 1. The isomers may interconvert by a trigonal twist of one ligand, whereby the CH_2 groups move from one side of the Co–N–quaternary C plane to the other. It was anticipated that the process would be rapid in solution and that the chiroptical data would have to be obtained in the solid state from a pure δδ (or λλ) $[Co(tame)_2]^{3+}$ salt. The demonstration of a Pfeiffer effect on addition of (+)-tartrate ion suggested that a resolution of the complex in the solid state could be achieved. This and the knowledge that the racemic isomer was more stable by 1.6 kcal mol^{-1} than the meso isomer from stain energy calculations made the prospect of a solid-state resolution feasible.

Experimental Section

The ligand 1,1,1-tris(aminomethyl)ethane (tame) was prepared by a modification of the method of Stetter and Bockmann.[21] Instead of attempting to collect the volatile free amine, the 1,1,1-tris(phthaliminodiethyl)ethane crystals (69 g, 0.14 mol) were shaken with potassium hydroxide (94 g, 1.68 mol) in water (250 ml) over a period of 24 h. The mixture was distilled to dryness (temperature <150 °C) and the tame distillate collected and neutralized with hydrochloric acid to yield tame·HCl. Water (50 ml) was then added to the residue in the distilling flask and the procedure repeated. The tame·HCl solutions were combined and evaporated to dryness over a steam bath. The white crystals were rubbed with methanol (50 ml), filtered off, and washed with methanol. The resulting leaflike crystals (6 g, 20%) decomposed above about 270 °C.

$[Co(tame)_2]Cl_3·H_2O$. tame·HCl (4.5 g, 0.02 mol) was dissolved in water (10 ml) and triturated with silver oxide (9.3 g, 0.04 mol) to release the amine and precipitate silver chloride. The mixture was filtered and the water solution of tame collected. Cobalt chloride (1.66 g, 0.007 mol) was dissolved in water (5 ml), to which hydrochloric acid (0.6 ml of 35%, 0.007 mol) and active charcoal (0.2 g) were added. The tame solution was added to this mixture and air was slowly drawn through the resulting solution (2 h) which turned orange-brown. It was then filtered into dilute hydrochloric acid (5 ml, 1 M) to prevent subsequent decomposition of the complex which occurred at room temperature for pH greater than 7. The solution was then concentrated on a rotary evaporator (60 °C and reduced pressure) and cooled in an ice bath to deposit bright orange hexagonal platelets. The crystals of $[Co(tame)_2]Cl_3·H_2O$ (1.45 g, 55%) were washed with ethanol and acetone and dried in an oven (70–80 °C). No chemical analysis was done, but the salt was characterized by UV–visible spectroscopy, by NMR, and by x-ray cell data. For $C_{10}H_{32}Cl_3CoN_6O$, mol wt 417.7, the space group is $P6_322$, and a = 7.48 (1) Å, c = 19.50 (3) Å, d_{measd} = 1.48 (1) g cm^{-3}, Z = 2, and d = 1.485 g cm^{-3}. The ligand has ^1H NMR resonances at 1.41 (CH_3) and 3.38 ppm (CH_2) and the chloride complex has corresponding resonances at 1.02 and 2.63 ppm with respect to TMS in D_2O.

$[Co(tame)_2]Cl[(+)_{589}$-*R*,*R*-tart]·5.4H_2O. The chloride salt (0.22 g, 0.55 mmol) was dissolved in water (10 ml) and triturated with fresh silver (+)-tartrate (0.2 g, 0.55 mmol) for 15 min. The mixture was filtered and the filtrate was reduced to 3 ml at the water pump and treated with a similar volume of ethanol. The solution was placed

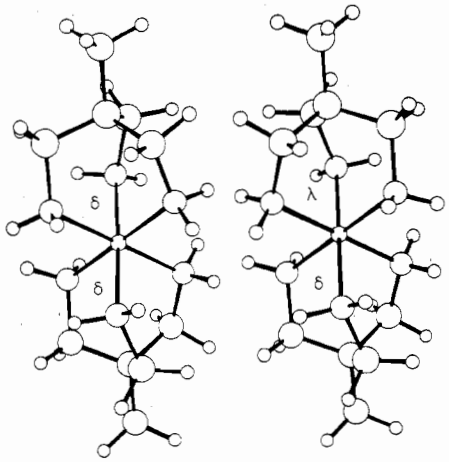

Figure 1. The $\delta\delta$ and $\lambda\delta$ isomers of $[Co(tame)_2]^{3+}$.

in a desiccator in vacuo over calcium chloride and large well-formed orange crystals were deposited over several days. Semimicro tests for both chloride and tartrate were positive and the crystals were further characterized by x-ray analysis.

Spectroscopy. UV and visible spectra were recorded on a Perkin-Elmer 402 spectrophotometer. ^1H NMR spectra were measured with a Varian T60 instrument. ORD measurements were obtained from a Perkin-Elmer 141MC spectropolarimeter with a quartz–iodine cycle tungsten lamp. CD spectra were recorded using a Roussel-Jouan Dichrograph II at the University of Queensland. Polystyrene disks for this technique were prepared by folding the finely ground crystals into polystyrene dissolved in benzene. The mixture was homogenized to a gum in air and solvent was removed in vacuo. This material was pressed at 50 ton/in.^{2} in a die heated at 60 °C and polished with rouge.

Crystal Data. The crystals were large chunky blocks elongated slightly along the *c* axis. Many were twins and the morphology showed the forms {110}, {010}, and {10$\bar{1}$}. The space group was obtained from precession photographs using Cu Kα radiation. The cell constants were refined[22] from the ψ and μ values (ψ and μ are the detector and equiinclination angles) of 52 high-angle reflections measured on a Stoe automatic Weissenberg diffractometer fitted with a graphite monochromator and using Mo Kα radiation. The space group is $P2_1$ with a = 14.631 (3) Å, b = 16.890 (3) Å, c = 8.720 (2) Å, and β = 143.9 (1)°. The measured density (by flotation) is 1.50 (1) g cm^{-3}; for $C_{14}H_{44.9}ClCoN_6O_{11.4}$ the formula weight is 574.7, and for Z = 2 the calculated density is 1.505 g cm^{-3}. The wavelength used was 0.7107 Å. The crystal used for data collection measured 0.30, 0.30, and 0.50 mm along the *a*, *b*, and *c* axis, respectively. It was mounted along the pseudo-*c* axis of a nonconventional body-centered cell defined for convenience. Data were collected by the ω-scan technique as described previously.[23] The constants in the variable-scan expression $\Delta\omega = A + B(\sin\mu/\tan(\psi/2))$ were 1.5–2.0 for A and 0.8 for B. Step increments of 0.01° were used with step times of 0.5 s for layers *hk*0–*hk*4 reducing to 0.2 s for layers *hk*5–*hk*12. Background counting time was 25 s. A total of 2692 unique reflections were recorded about the pseudo-*c* axis out to at least 50° in 2θ. A standard reflection, chosen on each layer, was measured every 30 reflections and showed no systematic change. Lorentz and polarization corrections were applied but no absorption corrections were made in view of the small regular nature of the crystal and low absorption coefficient (8.4 cm^{-1}). The transmission factors varied from 0.84 to 0.86 about the pseudo-*c* axis of rotation.

Structure Solution and Refinement

The cobalt and chlorine atom positions were found from a Patterson synthesis. These were then refined by a least-squares minimization of $\sum(|F_o| - |F_c|)^2$.[24] Besides the positional parameters and isotropic thermal parameters for the Co and Cl atoms, ten scale factors were refined for correct relative scaling of the single axis layers of data. A Fourier difference synthesis phased on the refined cobalt and chlorine positions revealed the presence of two superimposed mirror-image structures in the cell, a consequence of the pseudocenter introduced by the Co and Cl atoms having similar *y* coordinates. The correct image was determined unambiguously from stereochemical considerations and the relative weights of the mirror image peaks. The sites of all other nonhydrogen atoms in the $[Co(tame)_2]^{3+}$ and $(+)_{589}$-tartrate ions, as well as the oxygen positions of four ordered water molecules, were then located from this map. At this stage the tartrate ion was observed to be in the *S*,*S* configuration. The correct configuration for the structure was then obtained by inversion of all *y* coordinates to give the known[25] *R*,*R* configuration for the $(+)_{589}$-tartrate ion. A least-squares refinement of the scale factors, the atomic coordinates, and the individual isotropic thermal parameters converged with an R_1 index of 0.074. Anisotropic thermal parameters were then included in the refinement for all atoms, and the imaginary components of the scattering factors for Co and Cl were also introduced. Subsequent refinement involving these modifications was continued in alternate cycles of coordinate and anisotropic thermal parameter blocks and gave an R_1 value of 0.053. A second Fourier difference map then revealed the oxygen positions of three disordered water sites and the positions of all hydrogen atoms in the $[Co(tame)_2]^{3+}$ and tartrate ions. The three disordered oxygens were initially given atom multipliers based on the rough integration of electron density over 1-Å radius spheres surrounding the observed peak height positions. At this point the hydrogen atoms were included in the refinement with coordinates fixed in their observed positions and with fixed isotropic thermal parameters of 5.0 Å^2 for the methyl and hydroxyl hydrogens and 4.0 Å^2 for all others. The multipliers of the disordered oxygens and the hydrogen positions were included in the refinement which continued in cycles of three blocks to convergence with R_1 = 0.029. Finally, the hydrogen atom positions in all of the water molecules were determined from a third Fourier difference synthesis phased on the refined positions of all other atoms. The extensive hydrogen bonding in the structure proved a considerable aid in the search for their locations. The three water sites with reduced site occupancy factors showed no obvious positional or rotational disorder about the oxygen positions, although the hydrogen positions for two of these sites did. Two final sequences of least-squares refinement cycles were computed. Each sequence consisted of five blocks composed of (1) coordinates and anisotropic thermal parameters of all nonhydrogen atoms in $[Co(tame)_2]^{3+}$, (2) scale factors and coordinates of all atoms in $[Co(tame)_2]^{3+}$, (3) coordinates and anisotropic thermal parameters of all nonhydrogen atoms in the tartrate and chloride ions and the water molecules, (4) scale factors and coordinates of all atoms in the tartrate, chloride, and water entities, and (5) scale factors and coordinates of all nonhydrogen atoms in the structure. These blocks were necessary to obtain the appropriate final covariance data for the calculation of errors in the computed functions of structural coordinates and thermal parameters. This final refinement sequence reduced R_1 to 0.025 at convergence. The value of R_2 was 0.027. Unit weights were used in all refinements and the estimated error in an observation of unit weight was 0.77 from all refinement blocks in the final sequence. The average value of $(|F_o| - |F_c|)^2$, determined in ranges of $|F_o|$, was plotted vs. $|F_o|$ and $(\sin\theta)/\lambda$. The curves indicate a relative overweighting of the very strong and very weak reflections. The former curve varied randomly from 0.21 to 0.35 in the center ranges and had average values of 0.46 and 0.70 for the two terminal ranges. The latter curve showed a relatively flattened distribution over the $(\sin\theta)/\lambda$ ranges, with a variation from 0.20 to 0.56 over the complete curve and from 0.20 to 0.25 over the central angular ranges. These results indicated a satisfactory relative weighting scheme for the majority of reflections. A final difference map showed no peak height values larger than 0.2 e/Å^3 except for the region in the immediate vicinity of the cobalt atom, which showed several peaks from 0.2 to 0.35 e/Å^3 in height in the directions of the Co–N bonds. Typical water hydrogens appeared in earlier maps with peak heights of 0.25–0.35 e/Å^3, whereas hydrogens in the more rigid $[Co(tame)_2]^{3+}$ ion had peak heights varying from 0.30 to 0.55 e/Å^3.

In view of the observed charge delocalization over the whole complex ion in metal complexes,[26-28] the Co^+ scattering factors were used.[9] The factors for O, N, and C were taken from the same source, and for Cl^- the values of Doyle and Turner[30] were used. For hydrogen the values of Stewart[31] et al. were taken. Values of the anomalous components $\Delta f'$ and $\Delta f''$ in the scattering factors of Co (0.299, 0.973) and Cl (0.132, 0.159) were acquired from Cromer and Liberman.[32] The structure factors (electrons ×10, $P2_1$ indexed) and the root-mean-square amplitudes of vibration of the nonhydrogen atoms along the major axes of the thermal ellipsoids are available.[33] Table I contains the final atomic parameters.

Results and Discussion

Description of the Structure. Figures 2 and 3 show the

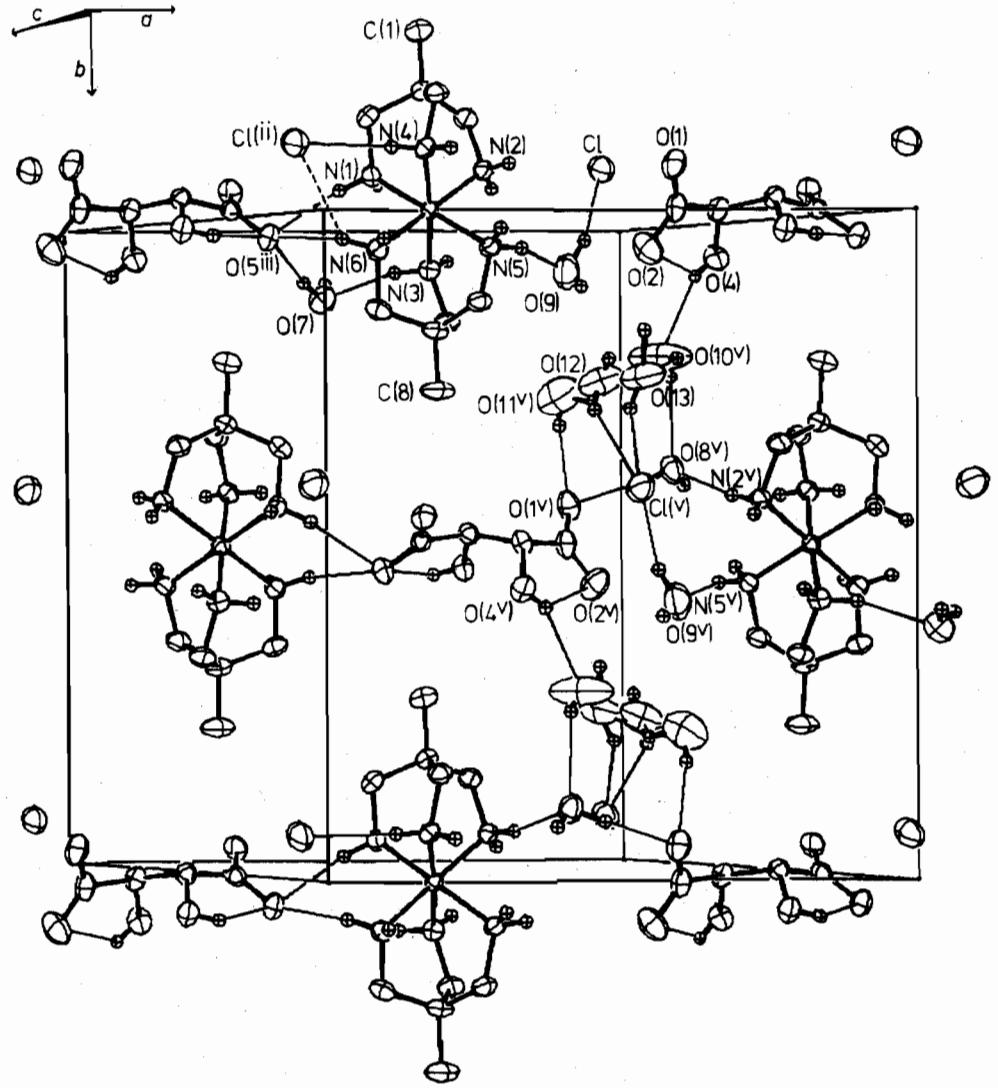

Figure 2. Unit cell of [λλ-[Co(tame)$_2$]Cl](*R*,*R*-tart)·5.4H$_2$O projected down *c**. Thermal ellipsoids contain 50% probability for nonhydrogen atoms. Symmetry transformations given as superscripts are defined in Table III.

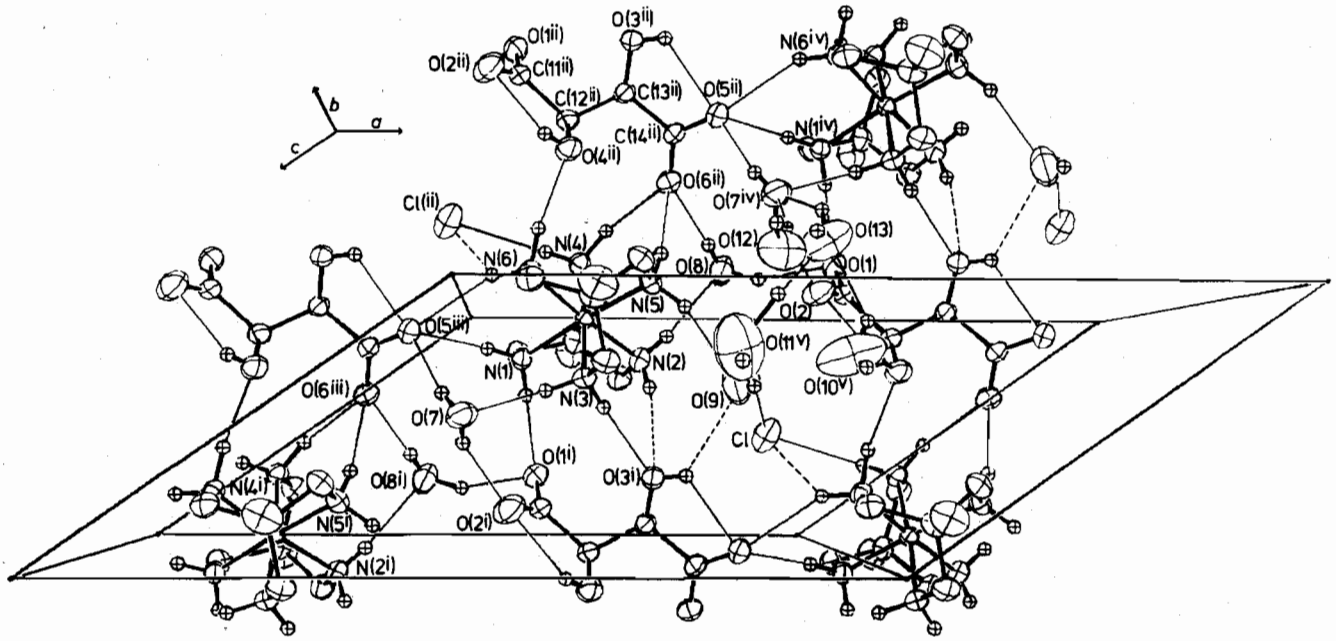

Figure 3. Unit cell of [λλ-[Co(tame)$_2$]Cl](*R*,*R*-tart)·5.4H$_2$O projected down *b*.

structure projected down the *c** and *b* directions, respectively. Tables II and III contain the molecular and crystal geometries. It is apparent from these that the threefold axis of [Co(tame)$_2$]$^{3+}$ is aligned approximately along the *b* axis, and the

Table I. Positional and Thermal Parameters[a] for [λλ-[Co(tame)$_2$]Cl](*R*,*R*-tart)·5.4H$_2$O

Atom[a]	*x*	*y*	*z*	β_{11}[d]	β_{22}	β_{33}	β_{12}	β_{13}	β_{23}
Co	1 810 (0)	0	38 (1)	524 (3)	152 (1)	1551 (10)	−4 (3)	721 (6)	12 (4)
Cl	7 368 (1)	−813 (1)	5363 (3)	1204 (14)	356 (5)	5475 (59)	−91 (7)	2132 (27)	−282 (13)
N(1)	1 687 (3)	−569 (2)	1841 (5)	698 (34)	206 (12)	2130 (103)	35 (16)	1022 (56)	61 (25)
N(2)	3 600 (3)	−659 (2)	1859 (6)	707 (34)	175 (12)	2577 (113)	6 (16)	1105 (59)	36 (26)
N(3)	3 125 (3)	809 (2)	2817 (5)	617 (33)	195 (12)	1714 (97)	−4 (15)	755 (53)	−14 (24)
N(4)	423 (3)	−808 (2)	−2714 (5)	642 (32)	195 (11)	1952 (100)	−56 (16)	874 (54)	−52 (24)
N(5)	2 034 (4)	590 (2)	−1597 (6)	983 (40)	168 (11)	2545 (111)	−60 (17)	1360 (63)	−49 (26)
N(6)	−41 (3)	644 (2)	−2001 (5)	678 (34)	198 (12)	2225 (106)	38 (16)	967 (56)	90 (26)
C(1)	2 258 (6)	−2710 (3)	1302 (9)	1611 (71)	201 (17)	4652 (212)	35 (28)	2295 (116)	164 (45)
C(2)	2 102 (4)	−1806 (2)	884 (7)	891 (46)	167 (14)	2790 (151)	−22 (20)	1312 (78)	17 (33)
C(3)	1 464 (4)	−1446 (2)	1493 (7)	1006 (48)	216 (15)	2795 (138)	−45 (21)	1411 (77)	63 (33)
C(4)	3 705 (4)	−1469 (2)	2682 (8)	863 (47)	203 (15)	2784 (147)	97 (22)	1231 (79)	195 (34)
C(5)	969 (5)	−1647 (2)	−1965 (8)	970 (50)	171 (14)	2654 (143)	−70 (20)	1288 (80)	−115 (32)
C(6)	3 085 (5)	1627 (2)	2120 (8)	1001 (53)	189 (15)	2420 (142)	−98 (22)	1202 (82)	−171 (32)
C(7)	1 507 (5)	1810 (2)	−756 (8)	1106 (55)	139 (14)	2597 (153)	50 (21)	1339 (85)	58 (33)
C(8)	1 356 (6)	2715 (3)	−1140 (10)	1975 (84)	152 (16)	4603 (216)	38 (29)	2434 (126)	86 (44)
C(9)	195 (4)	1516 (2)	−1516 (7)	877 (45)	199 (15)	2492 (135)	111 (20)	1096 (73)	104 (32)
C(10)	1 431 (4)	1425 (2)	−2442 (7)	1138 (51)	175 (13)	2663 (136)	−4 (21)	1455 (79)	64 (31)
O(1)	4 568 (3)	−586 (2)	−2679 (5)	812 (34)	412 (14)	3651 (113)	−179 (18)	1156 (59)	−237 (30)
O(2)	4 844 (3)	605 (2)	−1237 (6)	944 (39)	472 (17)	3737 (145)	113 (21)	1354 (70)	−85 (38)
O(3)	6 401 (3)	360 (2)	−2672 (5)	704 (30)	319 (11)	2109 (91)	111 (15)	963 (49)	298 (24)
O(4)	7 863 (3)	648 (2)	2422 (5)	811 (33)	326 (12)	2398 (100)	−73 (16)	1051 (54)	−257 (26)
O(5)	9 379 (3)	378 (2)	696 (5)	788 (32)	317 (12)	2706 (104)	−45 (16)	1190 (54)	8 (26)
O(6)	10 041 (3)	−405 (2)	3541 (5)	754 (32)	286 (12)	2285 (96)	123 (15)	983 (52)	200 (25)
C(11)	5 345 (3)	1 (4)	−1206 (5)	596 (33)	379 (15)	1804 (99)	20 (31)	810 (54)	81 (50)
C(12)	7 091 (4)	−33 (3)	833 (6)	646 (33)	259 (13)	1741 (92)	−63 (26)	821 (53)	−46 (42)
C(13)	7 355 (3)	−160 (2)	−506 (6)	584 (34)	202 (18)	1937 (110)	4 (16)	827 (59)	40 (25)
C(14)	9 068 (3)	−50 (3)	1402 (5)	589 (30)	176 (12)	2010 (97)	15 (22)	847 (51)	−15 (35)
				Water Oxygens					
O(7)	2 059 (3)	1212 (2)	4513 (6)	980 (38)	379 (14)	2966 (119)	−80 (19)	1231 (63)	−67 (31)
O(8)	2 865 (3)	−1127 (2)	−2502 (6)	1037 (39)	408 (15)	4173 (139)	157 (19)	1746 (70)	459 (35)
O(9)	5 600 (5)	835 (3)	3050 (8)	2255 (68)	594 (21)	6754 (206)	133 (32)	3538 (113)	338 (54)
O(10)	3 407 (6)	−2839 (3)	−1806 (11)	2575 (100)	343 (19)	7062 (294)	−6 (35)	1878 (146)	17 (57)
O(11)[b]	5 275 (21)	−2244 (9)	−1559 (36)	564 (44)	70 (7)	1702 (139)	53 (15)	872 (73)	60 (26)
O(12)	3 352 (8)	2605 (4)	−2632 (13)	2581 (154)	391 (31)	6101 (350)	−210 (55)	2959 (208)	61 (76)
O(13)	3 835 (15)	2534 (8)	−3086 (29)	1586 (192)	314 (55)	6600 (812)	−67 (82)	2059 (328)	107 (166)

Positional Parameters for the Hydrogen Atoms[c]

Atom	*x*	*y*	*z*	Atom	*x*	*y*	*z*	*B*, Å^2
			Cation Hydrogens					
H(1)	258 (6)	−50 (3)	355 (10)	H(2)	92 (5)	−34 (3)	139 (9)	4.0
H(3)	436 (6)	−43 (3)	315 (10)	H(4)	349 (5)	−72 (3)	73 (10)	4.0
H(5)	406 (6)	65 (3)	414 (10)	H(6)	280 (5)	84 (3)	339 (9)	4.0
H(7)	−38 (6)	−81 (3)	−323 (10)	H(8)	13 (5)	−76 (3)	−420 (10)	4.0
H(9)	310 (6)	58 (3)	−49 (10)	H(10)	157 (6)	35 (3)	−293 (10)	4.0
H(11)	−57 (5)	48 (3)	−187 (10)	H(12)	−88 (6)	54 (3)	−400 (10)	4.0
H(13)	306 (6)	−284 (3)	317 (11)	H(14)	263 (6)	−300 (3)	91 (10)	5.0
H(15)	125 (6)	−290 (3)	36 (10)	H(24)	127 (6)	298 (3)	−19 (11)	5.0
H(25)	215 (6)	289 (3)	−73 (10)	H(26)	29 (6)	281 (3)	−302 (10)	5.0
H(16)	187 (5)	−166 (3)	288 (10)	H(17)	44 (6)	−156 (3)	22 (10)	4.0
H(18)	429 (5)	−144 (3)	457 (9)	H(19)	436 (5)	−183 (3)	279 (10)	4.0
H(20)	143 (6)	−174 (3)	−245 (9)	H(21)	5 (5)	−199 (3)	−315 (9)	4.0
H(22)	330 (5)	196 (3)	336 (9)	H(23)	394 (6)	171 (3)	245 (10)	4.0
H(27)	37 (6)	159 (3)	−21 (10)	H(28)	−73 (5)	174 (3)	−297 (10)	4.0
H(29)	203 (5)	174 (3)	−238 (9)	H(30)	35 (6)	145 (3)	−421 (10)	4.0
			Tartrate and Water Hydrogens					
H(31)	687 (6)	45 (3)	−275 (10)	H(32)	722 (6)	93 (3)	187 (10)	5.0
H(33)	745 (5)	−48 (3)	174 (10)	H(34)	699 (5)	−69 (3)	−125 (9)	4.0
H(35)	269 (7)	94 (4)	577 (11)	H(36)	127 (7)	99 (4)	352 (11)	6.0
H(37)	366 (7)	−93 (4)	−208 (11)	H(38)	208 (6)	−90 (4)	−365 (11)	6.0
H(39)	590 (8)	105 (4)	315 (13)	H(40)	578 (7)	37 (4)	278 (12)	7.0
H(41)	387 (9)	−279 (5)	−33 (15)	H(42)	296 (9)	−254 (5)	−236 (16)	9.0
H(43)	580 (21)	−211 (12)	69 (42)	H(44)	496 (21)	−180 (11)	−219 (37)	10.0
H(45)	347 (13)	300 (7)	−337 (22)	H(46)	299 (13)	229 (7)	−363 (22)	8.0
H(47)	273 (29)	304 (18)	−367 (53)	H(48)	310 (24)	189 (42)	−458 (42)	8.0

[a] Positional parameters (×10^4). Anisotropic thermal parameters (×10^5) except for O(11) (×10^4). [b] O(11), O(12), O(13) are partially occupied water sites. They, as well as their hydrogens (43–48), were refined with site occupancy factors of 0.433, 0.686, 0.314, respectively. [c] Positional parameters (×10^3). Hydrogens were assigned fixed isotropic thermal parameters. [d] The form of the anisotropic temperature factor is $\exp[-(\beta_{11}h^2 + \beta_{22}k^2 + \beta_{33}l^2 + 2\beta_{12}hk + 2\beta_{13}hl + 2\beta_{23}kl)]$.

plane of the four carbons in the (+)$_{589}$-tartrate ion is approximately parallel to the *ac* plane. These ions interact through an intricate planar hydrogen-bond network which also entails the water molecules whose oxygens are O(7), O(8), and O(9). This molecular plane is parallel to the *ac* plane and is shown in projection in Figure 3. The two O(7)–H···O and two

Table II

Bond Lengths, Å

Ligand 1

Co–N(1)	1.970 (3)	N(4)–C(5)	1.493 (5)
Co–N(2)	1.974 (3)	C(3)–C(2)	1.524 (6)
Co–N(4)	1.966 (3)	C(4)–C(2)	1.529 (5)
N(1)–C(3)	1.495 (5)	C(5)–C(2)	1.528 (5)
N(2)–C(4)	1.495 (5)	C(2)–C(1)	1.544 (6)

Ligand 2

Co–N(3)	1.975 (3)	N(5)–C(10)	1.504 (5)
Co–N(6)	1.973 (3)	C(6)–C(7)	1.535 (5)
Co–N(5)	1.972 (3)	C(9)–C(7)	1.521 (6)
N(3)–C(6)	1.492 (5)	C(10)–C(7)	1.526 (6)
N(6)–C(9)	1.493 (5)	C(7)–C(8)	1.542 (6)

Bond Angles, Deg

Ligand 1

N(1)–Co–N(2)	90.07 (14)	N(4)–C(5)–C(2)	111.78 (31)
N(1)–Co–N(4)	88.03 (13)	C(3)–C(2)–C(4)	111.00 (33)
N(2)–Co–N(4)	88.81 (14)	C(3)–C(2)–C(5)	109.34 (32)
Co–N(1)–C(3)	117.82 (24)	C(4)–C(2)–C(5)	110.54 (32)
Co–N(2)–C(4)	117.17 (24)	C(3)–C(2)–C(1)	109.12 (36)
Co–N(4)–C(5)	117.77 (22)	C(4)–C(2)–C(1)	108.33 (35)
N(1)–C(3)–C(2)	111.82 (31)	C(5)–C(2)–C(1)	108.46 (35)
N(2)–C(4)–C(2)	111.78 (30)		

Ligand 2

N(3)–Co–N(6)	89.44 (13)	N(5)–C(10)–C(7)	111.70 (30)
N(3)–Co–N(5)	88.34 (13)	C(6)–C(7)–C(9)	110.32 (34)
N(6)–Co–N(5)	88.80 (14)	C(6)–C(7)–C(10)	109.28 (34)
Co–N(3)–C(6)	117.51 (22)	C(9)–C(7)–C(10)	111.03 (34)
Co–N(6)–C(9)	116.96 (23)	C(6)–C(7)–C(8)	108.43 (37)
Co–N(5)–C(10)	117.01 (25)	C(9)–C(7)–C(8)	108.67 (39)
N(3)–C(6)–C(7)	111.35 (31)	C(10)–C(7)–C(8)	109.06 (37)
N(6)–C(9)–C(7)	111.53 (32)		

Interligand Angles at Co, Deg

N(1)–Co–N(6)	92.53 (13)	N(3)–Co–N(2)	93.46 (14)
N(1)–Co–N(5)	177.15 (14)	N(3)–Co–N(4)	176.39 (14)
N(2)–Co–N(5)	88.73 (14)	N(6)–Co–N(4)	88.42 (13)
N(1)–Co–N(3)	89.16 (13)	N(4)–Co–N(5)	94.53 (13)
N(2)–Co–N(6)	176.14 (14)		

Tartrate Ion

Bond Lengths, Å

C(11)–O(1)	1.250 (6)	C(13)–C(14)	1.531 (4)
C(11)–O(2)	1.244 (6)	C(12)–C(13)	1.513 (5)
C(14)–O(5)	1.249 (4)	C(12)–O(4)	1.411 (5)
C(14)–O(6)	1.254 (4)	C(13)–O(3)	1.423 (4)
C(11)–C(12)	1.531 (4)		

Bond Angles, Deg

O(1)–C(11)–O(2)	126.69 (30)	C(11)–C(12)–C(13)	109.66 (26)
O(5)–C(14)–O(6)	125.65 (27)	C(12)–C(13)–C(14)	111.10 (25)
O(1)–C(11)–C(12)	116.15 (42)	C(11)–C(12)–O(4)	111.67 (37)
O(2)–C(11)–C(12)	117.15 (41)	C(13)–C(12)–O(4)	111.86 (31)
O(5)–C(14)–C(13)	117.60 (28)	C(12)–C(13)–O(3)	110.41 (29)
O(6)–C(14)–C(13)	116.75 (30)	C(14)–C(13)–O(3)	110.78 (28)

Torsion Angles,[a] Deg

Complex Cation

Co–N(1)–C(3)–C(2)	+26.7 (4)	Co–N(3)–C(6)–C(7)	+29.3 (4)
Co–N(2)–C(4)–C(2)	+29.0 (4)	Co–N(6)–C(9)–C(7)	+31.4 (4)
Co–N(4)–C(5)–C(2)	+27.6 (4)	Co–N(5)–C(10)–C(7)	+29.0 (4)
N(1)–C(3)–C(2)–C(1)	+164.4 (3)	N(3)–C(6)–C(7)–C(8)	+162.6 (4)
N(2)–C(4)–C(2)–C(1)	+162.5 (4)	N(6)–C(9)–C(7)–C(8)	+162.1 (3)
N(4)–C(5)–C(2)–C(1)	+164.7 (4)	N(5)–C(10)–C(7)–C(8)	+163.1 (4)
C(3)–C(2)–C(1)–H(13)	−66 (3)	C(6)–C(7)–C(8)–H(24)	−68 (3)
C(4)–C(2)–C(1)–H(14)	−61 (4)	C(9)–C(7)–C(8)–H(26)	−57 (3)
C(5)–C(2)–C(1)–H(15)	−69 (3)	C(10)–C(7)–C(8)–H(25)	−57 (3)
C(3)–C(2)–C(1)–H(25)	+50 (3)	C(6)–C(7)–C(8)–H(25)	+62 (3)
C(4)–C(2)–C(1)–H(13)	+55 (3)	C(9)–C(7)–C(8)–H(24)	+52 (3)
C(5)–C(2)–C(1)–H(14)	+59 (4)	C(10)–C(7)–C(8)–H(26)	+64 (3)

Tartrate Ion

O(1)–C(11)–C(12)–C(13)	+56.6 (5)	O(6)–C(14)–C(13)–C(12)	+48.5 (5)°
O(2)–C(11)–C(12)–O(4)	+1.3 (5)	O(6)–C(14)–C(13)–O(3)	+171.6 (3)
C(11)–C(12)–C(13)–C(14)	+169.9 (4)		

[a] The torsion angle about the bond J–K is the angle the bond K–L is rotated from the IJK plane. It is positive when, on looking from IJ to KL, the rotation is clockwise.

Table III. Apparent Hydrogen Bonds with the Complex Cation[a]

	N···B, Å	H···B, Å	N–H···B, deg
N(1)–H(1)···O(1)^{i}	2.835 (4)	1.96 (5)	168 (4)
N(1)–H(2)···O(5)^{iii}	3.083 (4)	2.17 (5)	170 (4)
N(2)–H(3)···O(3)^{i}	3.301 (4)	2.53 (5)	165 (4)
N(2)–H(4)···O(8)	3.103 (5)	2.25 (5)	166 (4)
N(3)–H(5)···O(3)^{i}	2.922 (4)	2.07 (5)	175 (4)
N(3)–H(6)···O(7)	2.967 (4)	2.06 (5)	165 (4)
N(4)–H(7)···Cl^{ii}	3.267 (3)	2.42 (5)	179 (4)
N(4)–H(8)···O(6)^{ii}	2.913 (4)	1.95 (5)	162 (4)
N(5)–H(9)···O(9)	3.103 (5)	2.20 (5)	155 (4)
N(5)–H(10)···O(6)^{ii}	3.052 (4)	2.23 (5)	167 (4)
N(6)–H(11)···O(5)^{iii}	3.111 (4)	2.31 (5)	147 (4)
N(6)–H(11)···Cl^{ii}	3.409 (3)	2.81 (5)	124 (4)
N(6)–H(12)···O(4)^{ii}	2.990 (4)	1.97 (5)	163 (4)
	O···B, Å	H···B, Å	O–H···B, deg
O(3)–H(31)···O(5)	2.630 (4)	2.16 (5)	120 (5)
O(3)–H(31)···O(9)^{iv}	2.978 (5)	2.50 (5)	122 (5)
O(4)–H(32)···O(2)	2.628 (4)	2.12 (5)	123 (5)
O(4)–H(32)···O(10)^{v}	2.942 (6)	2.26 (5)	147 (5)
O(7)–H(35)···O(2)^{i}	2.641 (4)	1.94 (6)	146 (6)
O(7)–H(36)···O(5)^{iii}	2.709 (4)	1.94 (6)	168 (6)
O(8)–H(37)···O(1)	2.772 (4)	1.87 (6)	157 (5)
O(8)–H(38)···O(6)^{ii}	2.723 (4)	1.94 (6)	174 (6)
O(9)–H(39)···O(10)^{v}	3.293 (8)	2.80 (6)	160 (9)
O(9)–H(40)···Cl	3.174 (6)	2.45 (6)	136 (5)
O(10)–H(41)···O(13)^{vi}	2.654 (14)	2.07 (7)	126 (6)
O(10)–H(42)···O(8)	2.930 (6)	2.40 (8)	144 (9)
O(11)–H(43)···O(13)^{vi}	3.117 (24)	1.79 (21)	151 (14)
O(11)–H(44)···O(1)	2.870 (16)	2.08 (18)	163 (19)
O(12)–H(47)···Cl^{v}	3.141 (6)	2.37 (25)	141 (14)
O(12)–H(46)···O(7)^{iv}	2.774 (7)	2.05 (12)	158 (10)
O(13)–H(45)···Cl^{v}	3.031 (13)	2.25 (11)	149 (10)
O(13)–H(48)···O(7)^{iv}	2.705 (13)	1.52 (23)	143 (14)

[a] Symmetry operations: (i) $x, y, z + 1$; (ii) $x - 1, y, z - 1$; (iii), $x - 1, y, z$; (iv) $x, y, z - 1$; (v) $1 - x, y + {}^1/_2, -z$; (vi) $1 - x, y - {}^1/_2, -z$.

O(8)–H···O hydrogen bonds between the water molecules and the carboxylate oxygens of the tartrate ions engender chains of end-to-end connected tartrate ions. These chains are bonded through the $[Co(tame)_2]^{3+}$ ion which forms numerous N–H···O hydrogen bonds with the water oxygens O(7), O(8), and O(9) and the carboxylate and hydroxyl oxygens of the tartrate ions. The $[Co(tame)_2]^{3+}$ ion also forms two N–H···Cl hydrogen bonds with the chloride ion. In fact every N–H hydrogen is involved in some close interaction with an oxygen atom or chloride ion. Only one bifurcated N–H hydrogen interaction is evident, and this is the N(6)–H(11) interaction with Cl^{ii} and O(5)^{iii}. The hydrogen bonding in the molecular plane parallel to *ac* is clearly indicated in Figure 3 and the dotted lines represent relatively weak hydrogen-bond interactions. Table III shows that the N···O distances range from 2.835 (4) to 3.301 (4) Å, a slightly larger range than that of the neutron diffraction distances listed by Hamilton and Ibers,[34] 2.87–3.07 Å, for unbranched bonds. Some of the N–H···O bonds observed here may be weakened by the multiple hydrogen-bonding interactions of the tartrate and water oxygens or the optimum packing hydrogen-bond arrangements which may not favor strong hydrogen bonds in all N–H···O encounters. The N–H···O angles for unbranched bonds range from 155 (4) to 175 (4)° and lie well within the range 119–175° determined from the neutron diffraction studies.[34] The N–H···O and N–H···Cl angles of the bifurcated interaction are 147 (4) and 124 (4)°. For the N–H···Cl interactions, the N···Cl distances of 3.267 (3) and 3.409 (3) Å lie within the range 3.15–3.48 Å established by the neutron diffraction. The N–H···Cl angles of 124 (4) and 179 (4)° lie on the outskirts of the literature range (122–171°).

The unforked hydrogen bonds involving the tartrate ions and the water oxygens O(7) and O(8) (Figure 3) have O···O distances and O–H···O angles ranging from 2.641 (4) to 2.772 (4) Å and from 146 (6) to 174 (6)°, respectively. The corresponding neutron diffraction ranges are 2.49–3.00 Å and 132–180° for unsymmetric unbranched O–H···O bonds. The tartrate hydroxyl groups appear to form bifurcated O–H···O bonds with an internal carboxylate oxygen and a water oxygen, O(9) and O(10) (see Figures 2 and 3). The internal O···O distances of 2.630 (4) and 2.628 (4) Å and the O···O(water) distances of 2.978 (5) and 2.94 (2) Å lie within the established range. The O–H···O angles of 120 (5)–147 (5)° are similar to those observed by neutron diffraction in other bifurcated systems. The other O–H···O hydrogen bonds involve the O–H bonds of the water whose oxygen is O(10) and the disordered waters with oxygens O(11), O(12), and O(13). These oxygens are O–H···O bonded between themselves to a carboxylate oxygen of the tartrate ion and to the water oxygens O(7) and O(8). Together with the O–H···Cl bonds formed by O(12) and O(13), each of the water oxygens O(10)–O(13) provides a direct or indirect hydrogen-bonded link between the molecular planes discussed above. The O–H···Cl interactions listed in Table III also have O···Cl distances and O–H···Cl angles not significantly different from the literature values[34] of 3.09–3.18 Å and 153–166°.

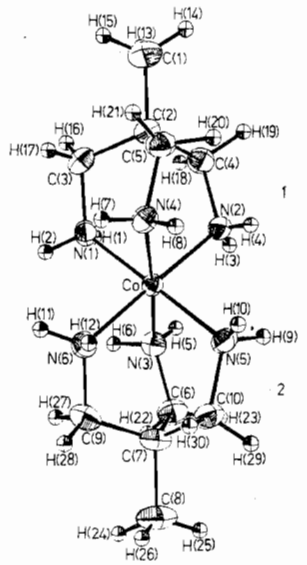

Figure 4. The λλ-$[Co(tame)_2]^{3+}$ ion with 50% probability thermal ellipsoids for the nonhydrogen atoms.

If the chloride ion has an ionic radius of 1.81 Å and the C, N, and O atoms have van der Waals (VDW) radii[35] of 1.7, 1.5, and 1.4 Å, there are no intermolecular nonbonded distances between the nonhydrogen atoms less than the sum of the VDW or VDW and ionic radii. For a hydrogen VDW radius of 1.2 Å there are only two intermolecular nonbonded contacts involving H atoms which are significantly less than the VDW radii sum. One of these is a C···H contact of 2.47 (6) Å (VDW radii sum is 2.9 Å) imposed on the carboxylate carbon, C(11), of the tartrate ion by the O(8)–H···O(1) (carboxylate oxygen) hydrogen bond. The other contact involves the same water oxygen O(8) and a methylene hydrogen on $[Co(tame)_2]^{3+}$ and is probaby imposed by N–H···O(8) hydrogen bonding (see Figure 3). The contact O(8)···H(20) of 2.37 (5) Å is not however inordinately less than the VDW sum of 2.6 Å.

The atoms of $[Co(tame)_2]^{3+}$ show the expected variations of their root-mean-square components of thermal vibration,[33] with the methyl carbons having the largest components approximately perpendicular to the pseudo-C_3 axis of the cation (see Figures 4 and 5). In the $(+)_{589}$-tartrate ion the largest

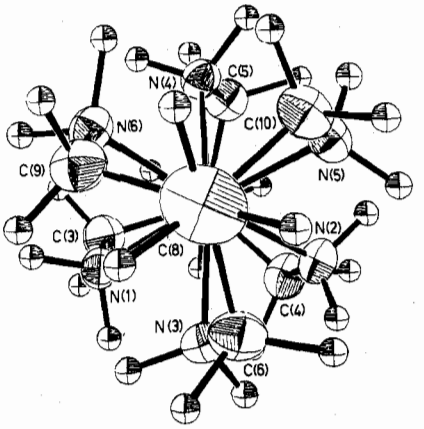

Figure 5. The λλ-$[Co(tame)_2]^{3+}$ ion viewed down the molecular threefold axis and showing a right-handed (Δ) screw sense.

components are approximately normal to the $CO–CO_2$ planes as expected (Figures 2 and 3). The water oxygens O(9)–O(13) have the largest vibration amplitudes and the weakly hydrogen-bonded oxygens O(10) and O(11) show exceptionally large values.

The Cation Geometry. The cation is shown in Figure 4 and in projection down the pseudo-threefold axis in Figure 5. The bond length and angles averaged over D_3 symmetry are given in Table IV. They are all normal for structures of this type[36,37] with the exception of the terminal C–C distances. Their mean length of 1.543 (4) Å increases to 1.560 (4) Å when corrected for thermal motion by the riding model which is significantly longer than the methylene to quaternary carbon bond distances. The mean N–H distance of 0.91 (2) Å observed here is slightly longer than the "optimal" value of 0.87 Å determined by Churchill[38] for x-ray N–H distances. The mean C–H length (excluding the methyl values which were not corrected for thermal motion) is found to be 0.99 (2) Å, again slightly longer than Churchill's "optimal" value of 0.95 Å.

The angular geometries of the two tame ligands are almost identical for angles related by the pseudo-twofold axis bisecting the N(1)–Co–N(3), N(4)–Co–N(5), and N(2)–Co–N(6) angles. These twofold related angles are tabulated in juxtaposition (Table II) for the nonhydrogen angles of the two ligands and all, except the N(1)–Co–N(2) and N(3)–Co–N(6) angles, are similar to within three standard deviations. Similarly, with the possible exception of the N–Co–N angles, the pseudo-threefold related angles of each ligand are equivalent, and the total nonhydrogen angular geometry of the complex conforms closely with D_3 symmetry. The mean angles N–Co–N, Co–N–C, N–C–C, and C–C–C of the chelate rings are 88.92 (6), 117.37 (10), 111.66 (13), and 110.25 (14)°, respectively. The equivalent angles in the quasi-D_3 complex $(-)_{546}$-$[Co(R,R\text{-ptn})_3]^{3+}$ (ptn is 2,4-diaminopentane), which has six-membered chelate rings similar to those of $[Co(tame)_2]^{3+}$, have the mean values 89.0 (3), 118.0 (4), 112.0 (6), and 117.2 (7)°.[37] Only the C–C–C angles differ significantly from those observed in $[Co(tame)_2]^{3+}$ and the closely tetrahedral value of 110.25 (14)° found here is probably imposed by the quaternary carbons. All angles in the $[Co(tame)_2]^{3+}$ complex involving hydrogen atoms are tetrahedral to within three standard deviations.

The CoN_6 core of the complex is distorted significantly from octahedral geometry, the main distortion being a relative trigonal twist of the donor groups N(1), N(2), N(4), and N(3), N(5), N(6) (see final section). This is probably caused by the repulsive hydrogen contacts H(2)···H(11), H(8)···H(10), and H(3)···H(5) (see Figure 4 and Table IV) and is in the correct sense to relieve such interactions. This twist increases the N(1)–Co–N(6), N(2)–Co–N(3), and N(4)–Co–N(5) angles to 92.53 (13), 93.46 (14), and 94.53 (13)°, respectively, from the octahedral value of 90° and correspondingly decreases the N(2)–Co–N(5), N(1)–Co–N(3), and N(6)–Co–N(4) angles. The six-membered chelate rings all have the λ conformation, describing the left-handed helix defined by the C···C(methylene) and N···N skew lines.[20] The conformation is intermediate between that of the regular skew boat and a boat ring and may be described as an asymmetric skew boat. Torsion angles are given in Table II and the skew-boat conformation is clearly indicated by the fact that all Co–N–C–C torsion angles have the same sign. The magnitudes of the C–C–C–H torsion are all 60° to within 3σ and indicate almost complete staggering of the methyl groups with respect to the opposing C–C bonds. The staggered conformation is also stabilized by minimizing H···H repulsive contacts with the methylene hydrogens and is illustrated in Figure 5.

Table IV. Comparison of Geometry of $[Co(tame)_2]^{3+}$ Isomers

Atoms	λλ(crystal)[a]	λλ	δλ
	Bond Lengths, Å		
Co–N(1)	1.972 (9)	1.963	1.969
N(1)–C(3)	1.495 (11)	1.498	1.498
C(3)–C(2)	1.527 (14)	1.516	1.516
C(2)–C(1)	1.543 (6)	1.517	1.517
	Bond Angles, Deg		
N(1)–Co–N(2)	88.9 (20)	89.92	89.58
N(1)–Co–N(3)	88.8 (7)	88.25	90.42
N(1)–Co–N(6)	93.5 (20)	91.97	90.42
N(1)–Co–N(5)	176.6 (7)	177.07	180.00
C(3)–N(1)–H(1)	107 (5)	108	108
C(3)–N(1)–H(2)	106 (10)	109	108
Co–N(1)–H(1)	107 (6)	106	107
Co–N(1)–H(2)	111 (11)	112	112
Co–N(1)–C(3)	117.4 (9)	115.2	115.2
N(1)–C(3)–C(2)	111.7 (4)	111.6	111.5
N(1)–C(3)–H(17)	109 (7)	110	110
N(1)–C(3)–H(16)	107 (8)	108	108
C(2)–C(3)–H(16)	113 (4)	110	110
C(2)–C(3)–H(17)	110 (10)	110	110
C(3)–C(2)–C(1)	108.7 (8)	108.8	108.8
C(3)–C(2)–C(4)	110.3 (18)	110.2	110.1
C(2)–C(1)–H(13)	110 (10)	110	110
	Close Contacts, Å		
N(1)···C(4)	2.82 (3)	2.78	2.77
H(1)···H(18)	2.49 (13)	2.34	2.33
H(1)···H(16)	2.12 (15)	2.22	2.21
H(2)···H(17)	2.13 (14)	2.27	2.26
H(2)···H(11)	2.24 (14)	2.12	2.10
H(1)···H(6)	2.31 (14)	2.28	2.10
	Torsion Angles, Deg		
Co–N(1)–C(3)–C(2)	+28.8 (47)	+32.5	33.0
N(1)–C(3)–C(2)–C(1)	+163.2 (26)	+160.7	160.4
C(3)–C(2)–C(1)–H(13)	−63 (12)	−64	64
C(3)–C(2)–C(1)–H(15)	+57 (7)	+56	56

[a] Values in parentheses are the ranges of symmetry-related geometries.

The Tartrate Ion. The $(+)_{589}$-tartrate ion is well illustrated in Figures 2 and 3. The mean carboxylate C–O bond length is 1.249 (3) and 1.266 (3) Å when corrected for thermal motion effects. As observed in the structure of ammonium tartrate[39] the chemically equivalent bond lengths in the tartrate ion are similar to within 3σ. The mean C–O(carboxylate) distance found in that tartrate structure was 1.252 (7) Å, uncorrected for thermal motion. The average C–C(carboxylate) distance of 1.531 (3) Å seen here is slightly longer than the central C(12)–C(13) value of 1.513 (5) Å. A similar effect was observed in the ammonium tartrate structure, the respective lengths being 1.542 (9) and 1.528 (13) Å, but the difference there is not significant. The mean value of 1.417 (3) Å for the C–O(hydroxyl) bond is similar to the value of 1.413 (9) Å in ammonium tartrate. In other tartrate

structures[40,41] chemically equivalent bond lengths have sometimes been found to differ. The chemically equivalent bond angles found here in $(+)_{589}$-tartrate are similar to within 4σ and not significantly different from those in ammonium tartrate. Angles involving hydrogen atoms do not differ significantly from the tetrahedral value. The mean O–H bond distance found in this structure is 0.79 (2) Å (averaged over O–H bonds in the tartrate and water molecules with oxygens O(7), O(8), and O(9)) and shows the expected shortening with respect to the N–H distance of 0.91 (2) Å. The CO_2–CO_2 sections of the tartrate ion are closely planar and twisted with respect to each other by 78.3 (2)°. The ammonium tartrate structure showed a similar twist of 62°.

Conformational Analysis. The potential energy of the isomers was computed by the strain energy formalism.[42-44] The strain energy U_{total} is represented by the summation $\sum U_{total} = \sum U_B + U_{NB} + \sum U_\theta + U_\phi$, where the terms are functions describing contributions from bond stretching, nonbonded interactions, angle deformation, and bond torsion, respectively. The form and parameterization of these contributions were, except for bond torsion,[45] those used previously.[46,47] Trial coordinates for each isomer were computed by Hilderbrant's procedure[48] which determines Cartesian coordinates from estimated internal geometry with the program CART. The energy minimization procedure[44,46] was carried out both with and without symmetry constraints[49] for each isomer with program MOL. Table IV contains the minimized asymmetric unit internal geometry for the two isomers and includes the D_3 averaged values for the λλ isomer in the crystal. The converged internal geometries resulting from the independent C_3-constrained and D_3-constrained refinements were identical and only the independent results are given here. The final coordinates of both conformers are available.[33] Table IV shows that the observed geometry of the λλ isomer in the crystal is accurately reproduced by the energy-minimized values despite the high accuracy of the structural analysis and the extensive hydrogen bonding of the N–H hydrogen atoms in the crystal.

The intra- and interligand close contacts are essentially identical in the observed and computed molecules, allowing for the slight reduction in the x-ray N–H (0.91 (2) Å) and C–H (0.99 (2) Å) bond lengths from the minimized values (0.99 and 1.06 Å). The torsion angles about the N–C and C–C bonds defining the chelate ring conformations are slightly more eclipsed in the observed structure (28.8 (2) and 163.2 (2)°; cf. 32.5 and 160.7° calculated). The observed relative staggering of the methyl groups about the C(1)–C(2) bonds is predicted in the computed molecules. The observed trigonal twist of the two tame ligands, exemplified here by the expansion of the N(1)–Co–N(6) type angles (93.5 (1)° crystal, 92.0° minimized) and the compression of the N(1)–Co–N(3) type angles (88.8 (1)° crystal, 88.3° computed), is similarly predicted by the molecular energy minimization and is caused by repulsive H(2)···H(11), H(1)···H(6), and symmetry-related contacts. These contact distances have the respective values 2.12 Å (0.6 kcal mol^{-1}) and 2.28 Å (0.3 kcal mol^{-1}). For the λδ-$[Co(tame)_2]^{3+}$ isomer, the minimized configuration has C_{3i} symmetry and necessarily there is no relative twist of the two ligands. The N–H···H–N interligand contacts in this case merely serve to maintain the interligand angles near their octahedral values.

The final strain energies of the λλ-$[Co(tame)_2]^{3+}$ and λδ-$[Co(tame)_2]^{3+}$ isomers are 26.9 and 28.5 kcal mol^{-1} (Table V) for the complete molecules. From the subdivision in terms of the net U_B, U_{NB}, U_θ, and U_ϕ energies given in Table V and the above discussion, it is apparent that the major part of the total energy difference of 1.6 kcal mol^{-1} resides in the interligand N–H···N–H nonbonded interaction terms. Thus in λδ-$[Co(tame)_2]^{3+}$ the H(1)···H(6) type interactions contribute six terms of 0.7 kcal mol^{-1} (total 4.2 kcal mol^{-1}), whereas in λλ-$[Co(tame)_2]^{3+}$ the H(2)···H(11) and H(1)···H(6) type contacts contribute three terms each of 0.6 and 0.3 kcal mol^{-1} (total 2.7 kcal mol^{-1}). It is also evident from Table V that the isomeric energy differences are similar for the complete and reduced molecules, although for comparative refinements in which the torsion energies were defined as functions of only one of the nine torsion angles the energy difference is only 1.4 kcal mol^{-1}.

Table V. Final Strain Energies[a] of the $[Co(tame)_2]^{3+}$ Isomers

Conformer	Refinement	ΣU_B	ΣU_{NB}	ΔU_θ	ΣU_ϕ	U_{total}
δδ	Independent[b]	2.07	13.57	4.61	6.64	26.90
δδ	Independent 2[c]	1.76	11.83	4.43	6.64	24.66
δδ	C_3 constrained[c]	1.77	11.89	4.37	6.63	24.67
δδ	D_3 constrained[c]	1.77	11.89	4.37	6.64	24.67
δδ	Independent 3[d]	1.81	12.00	4.18	7.15	25.14
λδ	Independent 1[b]	2.37	15.09	4.26	6.77	28.49
λδ	Independent 2[c]	2.09	13.34	4.07	6.77	26.27
λδ	Independent 3[d]	2.13	13.53	3.78	7.12	26.56

[a] All energies in kcal mol^{-1}. [b] Whole molecule. [c] Methyl groups omitted. [d] In these refinements the intrinsic torsion energies about the bonds were defined as functions of only one of the nine torsion angles.

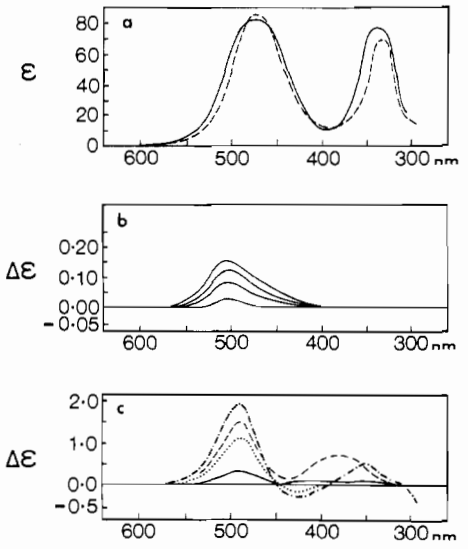

Figure 6. (a) Visible absorption spectra of $[Co(tame)_2]Cl_3$ (—) and $[Co(en)_3]Cl_3$ (---) in water. (b) CD curves of $[Co(tame)_2]Cl_3$ 0.01 M in aqueous $K_2[(+)_{589}$-tart] at concentrations of 0.01, 0.044, 0.22, and 1.06 M. (c) CD spectra of $[(+)_{589}$-$[Co(en)_3]Cl[(+)_{589}$-tart]·xH_2O (---) and [λλ-$[Co(tame)_2]Cl][(+)_{589}$-tart]·5.4HO (—) in a polystyrene disk, $(+)_{589}$-$[Co(en)_3]Cl_3$ in aqueous solution (- · - ·), and $[Co(en)_3]Cl_3$·$3H_2O$ in a KBr disk (····).

Optical Activity. The spectral properties of $[Co(tame)_2]^{3+}$ and $[Co(en)_3]^{3+}$ ions are compared in Figure 6. The absorption spectra are similar and for $[Co(tame)_2]Cl_3$ ϵ_{max} for the 472 nm $^1A_{1g} \rightarrow {}^1T_{1g}$ transition is 81 cm^2 mol^{-1}. Because the $[Co(tame)_2]^{3+}$ conformers equilibrate in solution, we have recorded the CD (circular dichroism) spectra as finely ground and dispersed powders in polystyrene. The solid-state CD spectrum of $[Co(tame)_2]Cl[(+)_{589}$-tart]·$5.4H_2O$ in a polished polystyrene disk shows a single large positive peak under the $^1A_{1g} \rightarrow {}^1T_{1g}$ absorption band envelope of the $Co^{III}N_6$ chromophore. Polystyrene disks were employed to avoid the possibility of conformational isomerization on forming a solid solution in a KBr disk. The similarity between the solid-state visible CD spectra of $(+)_{589}$-$[Co(en)_3]Cl$·$3H_2O$ and $[(+)_{589}$-$[Co(en)_3]Cl][(+)_{589}$-tart]·xH_2O indicates that the contribution to the complex ion CD from the dissymetric

influence of the tartrate ion is considerably lower in magnitude than the intrinsic molecular effect. Hence the CD exhibited by the $[Co(tame)_2]Cl[(+)_{589}\text{-tart}]\cdot 5.4H_2O$ crystals in the $^1A_{1g} \rightarrow {}^1T_{1g}$ absorption region should be largely representative of the λλ configuration of the complex $[Co(tame)_2]^{3+}$ ion. Other CD studies of symmetrical Co(III) complex cations, in solid and solution media containing optically active counteranions,[50-53] have shown that the optical activity induced in these complexes by the dissymmetric environments is generally an order of magnitude less than that observed here for $[Co(tame)_2]^{3+}$ and $(+)_{589}\text{-}[Co(en)_3]^{3+}$.

Relatively large changes induced in the visible solution CD spectra of $[Co(diamine)_3]^{3+}$ complexes by certain polarizable oxy anions (e.g., PO_4^{3-} and SeO_3^{2-})[54-62] have sometimes been attributed[56,58,63] to specific ion-pair formation through hydrogen bonding between the oxy anion and preferred conformational isomers. In some cases (e.g., $(+)_{589}\text{-}[Co(en)_3]^{3+}$ and $(+)_{589}\text{-}[Co((+)_{589}\text{-pn})]^{3+}$; pn is 1,2-diaminopropane), the ion pairing has been considered to modify the d–d transition rotatory strengths in the preferred complex conformer, either by mixing with a new charge-transfer transition generated by the ion-pair complex[56,57] or by the dissymmetry associated with new asymmetric centers at the nitrogen donors.[60] In others (e.g., $(+)_{589}\text{-}[Co(tn)_3]^{3+}$; tn is 1,3-diaminopropane), it was thought that the visible solution CD spectral changes reflected a variation in conformer proportions resulting from the specific ion pairing rather than electronic changes in the associated conformers.[54,64] In the crystalline $[Co(tame)_2]Cl(+)_{589}\text{-tart}]\cdot 5.4H_2O$ salt, the complex cation is elaborately hydrogen bonded to surrounding $(+)_{589}$-tartrate and water molecules. However, as implied above from the studies of tartrate influence on symmetric Co(III) complexes[52,53] and from the similarity between the solid-state visible CD spectra of $(+)_{589}\text{-}[Co(en)_3]^{3+}$ in various halide environments[65] and that in a preferred $(+)_{589}$-tartrate environment, it is assumed here that the outer-sphere $(+)_{589}$-tartrate perturbations on the visible CD of $[Co(tame)_2]^{3+}$ are considerably less than the observed visible CD of the $[Co(tame)_2]Cl[(+)_{589}\text{-tart}]\cdot 5.4H_2O$ compound.

The CD curve for $[Co(tame)_2]^{3+}$ in aqueous $(+)_{589}$-tartrate solution indicates a substantial Pfeiffer effect[66] in the visible spectral region (Figure 6b). This has the same sign as observed in the crystal spectrum and it is tempting but not necessary to conclude that in solution with $(+)_{589}$-tartrate the $\lambda\lambda \rightleftarrows \delta\delta$ equilibrium is shifted to the left. Both the crystal and the $(+)_{589}$-tartrate solution of the complex ion give $(+)_{589}$ signs in CD and ORD and phenomologically the complex in the crystal can be described as $(+)_{589}$-λλ. Inspection of the C_3 view of the complex (Figure 5) shows it to form a right-handed helix and the complex ion may be fully designated $(+)_{589}$-$\Delta\lambda\lambda$-$[Co(tame)_2]^{3+}$.

Correlation of Observed and Computed CD. The geometry and absolute configuration of the CoN_6 core are relevant to the evaluation of the optical activity models of Piper and Karipides[1,2] and of Richardson.[3-5,16-18] The $Co^{III}N_6$ chromophore of λλ-$[Co(tame)_2]^{3+}$ observed in the crystal structure is depicted in Figure 7 as a projection onto the plane perpendicular to the pseudo-C_3 axis of the complex ion. The trigonal twist angles, ω, were here defined by donor atom pairs having the chiral sense of a Δ tris(bidentate) complex and are shown with the polar angles, θ, subtended by the six Co–N bonds at the C_3 axis. The pseudo-C_3 axis was defined by the perpendicular (through the Co atom) to the average of the donor atom planes N(1), N(2), N(4) and N(3), N(5), N(6), and the trigonal-twist angles were determined from the projections of the appropriate Co–N bonds on this mean plane. The results for cobalt tame and en complexes are compared with the octahedral values in Table VI. For $\Delta\lambda\lambda$-$[Co(tame)_2]^{3+}$ the chromophore configuration is equivalent to that of a Δ tris(bidentate) complex having an azimuthal contraction ($\omega > 60°$) and an insignificant polar or trigonal elongation ($\theta < 54.74°$) of the $Co^{III}N_6$ core.

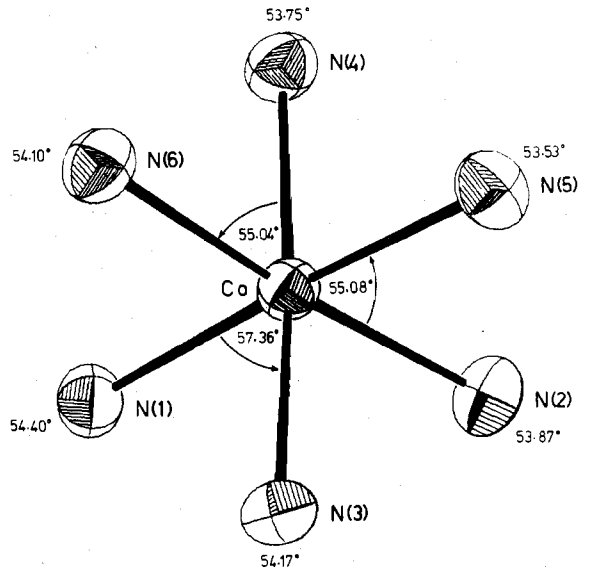

Figure 7. The $Co^{III}N_6$ core of λλ-$[Co(tame)_2]^{3+}$ in projection down the molecular threefold axis.

Table VI. $Co^{III}N_6$ Core Geometry

Complex	ω,[a] deg	θ,[a] deg	Ref
$\Delta\lambda\lambda$-$[Co(tame)_2]^{3+}$	55.8 (23)	54.0 (9)	*d*
λλ-$[Co(tame)_2]^{3+}$	56.8	54.7	*b*
$\delta\lambda$-$[Co(tame)_2]^{3+}$	60.0	54.4	*b*
$\Delta\lambda\lambda\lambda$-$[Co(en)_3]^{3+}$	54.9 (23)	55.9 (6)	*e*
λλλ-$[Co(en)_3]^{3+}$	56.2	54.9	*b, c*
Octahedron	60	54.74	

[a] See text for angle definitions, errors are the esd's of three independent values. [b] From energy minimization calculations. [c] K. R. Butler, P. F. Crossing, and M. R. Snow unpublished calculations. [d] This crystal study. [e] Reference 71; $Cl_3\cdot H_2O$ salt.

The signs of the rotary strengths for the $^1A_1 \rightarrow {}^1A_2$ and $^1A_1 \rightarrow {}^1E$ transitions of a D_3 $Co^{III}N_6$ chromophore are predicted from the first-order crystal field model of Piper and Karipides[1] to be determined by the equation

$$R' = \pm ez(3/7)(35\pi)^{1/2} \sin^3\theta \sin 3\delta$$

where +, − refer to the $^1A_1 \rightarrow {}^1E$ and $^1A_1 \rightarrow {}^1A_2$ bands. The term δ is $\pm(60 - \omega)$ where the positive and negative signs refer to the Δ and Λ configurations, respectively. In the present analysis the observed CD[67-69] for the ^1E band of $\Lambda(+)_{589}$-$[Co(en)_3]^{3+}$ is used as a reference to define the absolute sign for R'. This complex, which has $\omega < 60°$ and $\delta < 0°$ in crystalline environments,[70,79] exhibits a large positive rotatory strength for the $^1A_1 \rightarrow {}^1E$ chromophore transition. The above expression for R' then gives the correct sign for the observed CD bands of $\Lambda(+)_{589}$-$[Co(en)_3]^{3+}$ if the donor atom charge z is positive as will be assumed here. Evidence for charge delocalization in complex ions[26,27] indicates that this situation may be physically approached but is probably unrealistic because of the relatively large negative charges on the nitrogen atoms in uncomplexed amino groups. However, this is unimportant when predicting the rotatory strengths of complexes with chromophores similar to that of the reference.

The distortion constant (δ) for the $\Delta\lambda\lambda$-$[Co(tame)_2]^{3+}$ chromophore is determined from the mean ω value of 55.83° to be +4.17°, and the configuration is essentially the mirror image of that for the chromophore generally observed in crystal structures of Λ-$[Co(en)_3]^{3+}$ which has $\delta < 0°$. The expression for R' then indicates a negative rotatory strength for the $^1A_1$

$\rightarrow {}^1E$ component of the ${}^1A_{1g} \rightarrow {}^1T_{1g}$ absorption band of the observed $\lambda\lambda$-$[Co(tame)_2]^{3+}$ chromophore. Similarly a positive rotatory strength is predicted for the ${}^1A_1 \rightarrow {}^1A_2$ transition. If the single positive band observed in the solid-state visible CD spectrum of $\lambda\lambda$-$[Co(tame)_2]^{3+}$ is indeed the composite of a dominant[80,81] ${}^1E$ band and a recessive ${}^1A_2$ band, Piper's model is refuted, and the nodal properties of the rotatory strengths in D_3 complexes are not trivially determined on the basis of a first-order crystal field model of the ML_6 chromophore. However there is some evidence, both experimental and theoretical, to suggest that the ${}^1A_2$ CD component of the ${}^1A_{1g} \rightarrow {}^1T_{1g}$ octahedral transition may possibly dominate in this complex.

The effect of phosphate ion on the aqueous solution visible CD spectra of the complex ions $(+)_{589}$-$[Co(en)_3]^{3+}$,[55-59] $(+)_{589}$-$[Co((+)pn)_3]^{3+}$,[55,57] and Δ-$(-)_{589}$-$[Co((+)chxn)_3]^{3+}$ (chxn is 1,2-cyclohexaminediamine)[60] was described in terms of an enhancement of the ${}^1A_1 \rightarrow {}^1A_2$ and a reduction of the ${}^1A_1 \rightarrow {}^1E$ component rotatory strengths under the low-energy ${}^1T_{1g}$ absorption band envelope. This was attributed[56,58,60,63] to the $[Co(diamine)_3]^{3+}$–PO_4^{3-} ion-pair interaction, and assignment of the CD bands was inferred from the identification[65,82] of the ${}^1A_2$ and ${}^1E$ bands observed in the visible CD spectrum of aqueous $(+)_{589}$-$[Co(en)_3]^{3+}$. The visible CD spectrum of $(+)_{589}$-$[Co(sen)]^{3+}$, where sen is the sexadentate ligand $CH_3C(CH_2NHCH_2CH_2NH_2)_3$, was found[60] to be remarkably similar in form to the spectra of the above tris(diamine) complexes in phosphate ion solution. Since the $[Co(sen)]^{3+}$ complex consists of a $[Co(en)_3]^{3+}$ substrate trigonally capped by $CH_3C(CH_2-)_3$, the assignment of the low-energy trigonal CD components was again based on the $[Co(en)_3]^{3+}$ results.[65,82] The higher energy dominant negative CD component under the ${}^1A_{1g} \rightarrow {}^1T_{1g}$ envelope of $(+)_{589}$-$[Co(sen)]^{3+}$ was consequently ascribed to the ${}^1A \rightarrow {}^1A$ transition of this ideally C_3 symmetric complex, and the $[Co(sen)]^{3+}$ complex was regarded as a model for the $[Co(diamine)_3]^{3+}$,PO_4^{3-} ion pair in speculation on the origin of the observed CD changes in phosphate ion solutions.[60] If these conjectures are correct and the ${}^1A$ band is dominant in the CD spectrum of the trigonally capped complex, then the single positive CD peak observed for $[Co(tame)_2]^{3+}$ under the ${}^1A_{1g} \rightarrow {}^1T_{1g}$ envelope may well be composed of a dominant ${}^1A_2$ band and a recessive ${}^1E$ band. Here the tame ligands simulate the $CH_3C(CH_2NH-)_3$ trigonal cap of $[Co(sen)]^{3+}$, but the asymmetric nitrogen centers, proposed[60] to be the major source of differences between the visible CD spectra of $(+)_{589}$-$[Co(sen)]^{3+}$ and $(+)_{589}$-$[Co(en)_3]^{3+}$, are absent in the $[Co(tame)_2]^{3+}$ complex. If the lower order environmental effects are disregarded, the sole source of dissymmetry and optical activity in the solid-state structure of $[Co(tame)_2]^{3+}$ is the conformation of the six-membered Co–tame chelate rings. The visible CD spectra of aqueous $(+)_{589}$-$[Co(sen)]^{3+}$ and solid-state $\lambda\lambda$-$[Co(tame)_2]^{3+}$ are comparable in magnitude allowing for the decrease in intensity of the disk spectrum due to depolarization of the circularly polarized light.[65] It then seems apparent that the spectrum observed[60] for $(+)_{589}$-$[Co(sen)]^{3+}$ and possibly those found[56-60] for the above $[Co(diamine)_3]^{3+}$ complexes in phosphate solution could be largely influenced (if not dominated) by the contributions arising from preferred conformations of the trigonal caps. These may be induced by the minimization of steric interactions with the cobalt–diamine chelate rings, although the relative energies of the possible conformers have not been estimated.

In the CD spectrum of aqueous $(-)_{589}$-$[Co((+)cptn)_3]Cl_3$[83,84] (cptn is 1,2-cyclopentanediamine), the higher energy dominant negative component in the ${}^1A_{1g} \rightarrow {}^1T_{1g}$ absorption band region was also attributed[83] to the ${}^1A_1 \rightarrow {}^1A_2$ transition of the D_3 complex chromophore. Similarly the dominant positive component in the same region of Δ-$(+)_{589}$-$Co(tmd)_3Br_3$ (tmd is 1,4-diaminobutane) has been assigned to the ${}^1A_1 \rightarrow {}^1A_2$ transition.[85] Although the CD of these complexes may not be directly relevant to that of $[Co(tame)_2]^{3+}$, the assignments, if correct, provide further evidence that the ${}^1E$ CD band under the ${}^1T_{1g}$ envelope is not always dominant in D_3 cobalt(III)–polyamine complexes.

The one-electron crystal field model of Richardson,[3] which predicts the *net* rotatory strength for the ${}^1A_{1g} \rightarrow {}^1T_{1g}$ transition of a D_3 symmetric Co(III) complex to second order in perturbation theory, also offers some conjectural support for the dominance of the ${}^1A_1 \rightarrow {}^1A_2$ trigonal component in the CD spectrum of $[Co(tame)_2]^{3+}$. For ligand perturbing sites having positively signed charges, the model implies a dominant ${}^1A_2$ trigonal compnent in the *net* rotatory strength of the ${}^1A_{1g} \rightarrow {}^1T_{1g}$ transition when the polar coordinates of the perturbers lie in the range $\theta > 54.74°$ or $\theta > 125.26°$, as observed for the majority of the ligand atoms in the $[Co(tame)_2]^{3+}$ complex. This inference is based on the observation that for $(+)_{589}$-$[Co(en)_3]^{+}$, where the corresponding atom types lie on the opposite side of the nodal polar angle (54.74°), the ${}^1E$ band is dominant[65,82] (the a priori prediction of the model[3] when the perturbers with $125.26° > \theta > 54.74°$ are assumed to have positive charges). The result should not be affected if the donor atom charges are negative, even when the nonligating atoms are included (as in the Richardson model) in the expressions for the *net* and component rotatory strengths. But this assumes that the relative magnitudes of the contributions from the nonligators and the donor atoms are similar for the two complexes and that the polar dispositions of the atoms in each of these groups are on opposing sides of the nodal polar angle of 54.74° in $[Co(tame)_2]^{3+}$ and $(+)_{589}$-$[Co(en)_3]^{3+}$. The model then predicts qualitatively that the ${}^1A_2$ component should be dominant in the ${}^1A_1g \rightarrow {}^1T_{1g}$ transition rotatory strength for $[Co(tame)_2]^{3+}$ if the ${}^1E$ band has the dominant CD in $(+)_{589}$-$[Co(en)_3]^{3+}$.

If the above evidence for the dominance of the ${}^1A_1 \rightarrow {}^1A_2$ rotatory strength under the ${}^1T_{1g}$ band envelope in the CD spectrum of $[Co(tame)_2]^{3+}$ is accepted, then the observed positive CD band in this region supports the model of Piper and Karipides which, as delineated above, predicts the CD for the ${}^1A_2$ band to be positive from the observed structural geometry. Nevertheless this first-order crystal field model remains untested by the CD of the $[Co(tame)_2]^{3+}$ complex until the symmetry of the dominant CD band in the visible spectral region is positively identified.

Acknowledgment. We are pleased to acknowledge the assistance of Dr. C. J. Hawkins in obtaining the polystyrene-disk CD spectra. Financial support from the Australian Research Grants Committee and the award of a Commonwealth Postgraduate Award (to R.J.G.) is gratefully acknowledged.

Registry No. $[Co(tame)_2]Cl_3$, 60909-16-2; $[Co(tame)_2]Cl$-$[(+)_{589}$-*R*,*R*-tart], 60934-83-0.

Supplementary Material Available: Tables of rms amplitudes of vibration of non-H atoms along the major axis of thermal ellipsoids, structure factor amplitudes, and orthogonal coordinates and views of $[Co(tame)_2$-$\delta\delta]^{3+}$ and $[Co(tame)_2$-$\lambda\delta]^{3+}$ perpendicular to the C_3 axis (15 pages). Ordering information is given on any current masthead page.

References and Notes

(1) T. S. Piper and A. Karipides, *Mol. Phys.*, **5**, 475 (1962).
(2) A. Karipides and T. S. Piper, *J. Chem. Phys.*, **40**, 674 (1964).
(3) F. S. Richardson, *J. Phys. Chem.*, **75**, 692 (1971).
(4) F. S. Richardson, *Inorg. Chem.*, **11**, 2366 (1972).
(5) R. W. Strickland and F. S. Richardson, *Inorg. Chem.*, **12**, 1025 (1973).
(6) W. Moffitt, *J. Chem. Phys.*, **25**, 1189 (1956).
(7) S. Sugano, *J. Chem. Phys.*, **33**, 1883 (1960).
(8) N. K. Hamer, *Mol. Phys.*, **5**, 339 (1962).
(9) H. Poulet, *J. Chim. Phys. Phys.-Chim. Biol.*, **59**, 584 (1962).

(10) A. J. McCaffery and S. F. Mason, *Mol. Phys.*, **6**, 359 (1963).
(11) T. Bürer, *Mol. Phys.*, **6**, 541 (1963).
(12) A. D. Liehr, *J. Phys. Chem.*, **68**, 665 (1964).
(13) A. D. Liehr, *J. Phys. Chem.*, **68**, 3629 (1964).
(14) M. Shinada, *J. Phys. Soc. Jpn.*, **19**, 1607 (1964).
(15) C. E. Schäffer, *Proc. Roy. Soc. London, Ser. A*, **297**, 96 (1968).
(16) F. S. Richardson, *J. Chem. Phys.*, **54**, 2453 (1971).
(17) F. S. Richardson, *Inorg. Chem.*, **10**, 2121 (1971).
(18) R. W. Strickland and F. S. Richardson, *J. Chem. Phys.*, **57**, 589 (1972).
(19) S. F. Mason, *J. Chem. Soc A*, 667 (1971).
(20) Commission on Nomenclature of Inorganic Chemistry, *Inorg. Chem.*, **9**, 1 (1970); *I.U.P.A.C., Inf. Bull., Append. Tentative Nomencl., Symb., Units, Stand.*, **No. 33**, 68 (1973).
(21) H. Stetter and W. Bockmann, *Chem. Ber.*, **84**, 834 (1951).
(22) Program SUUCLS by M. Barnet, The University of Sydney, 1966.
(23) M. R. Snow, *Acta Crystallogr., Sect. B*, **30**, 1850 (1974).
(24) F_o and F_c are the observed and calculated structure factors. $R_1 = \sum||R_o| - |F_c||/\sum|F_o|$; $R_2 = [\sum(|F_o| - F_c|)^2/\sum|F_o|^2]^{1/2}$. The error in an observation of unit weight is defined as $[\sum(|F_o| - |F_c|)^2/(N_{obs} - N_{var})]^{1/2}$. In addition to local programs for the University of Adelaide CDC 6400, the following programs or modifications were used: Zalkin's FORDAP Fourier program; FUORFLS, a modification by Taylor of Busing, Martin, and Levy's ORFLS program; ORFFE, a function and error program by Busing, Martin, and Levy; Blount's geometry program BLANDA; Johnson's ORTEP, a thermal ellipsoid plot program.
(25) J. M. Bijvoet, A. F. Peerdeman, and A. J. Van Bommel, *Nature (London)*, **168**, 271 (1951).
(26) K. N. Raymond, D. W. Meek, and J. A. Ibers, *Inorg. Chem.*, **7**, 1111 (1968).
(27) A. Kobayashi, F. Marumo, and Y. Saito, *Acta Crystallogr., Sect. B.*, **28**, 2709 (1972).
(28) M. Iwata and Y. Saito, *Acta Crystallogr., Sect. B*, **29**, 822 (1973).
(29) "International Tables for X-Ray Crystallography", Vol. III, Kynoch Press, Birmingham, England, 1968.
(30) P. A. Doyle and P. S. Turner, *Acta Crystallogr., Sect. A*, **24**, 390 (1968).
(31) R. F. Stewart, E. R. Davidson, and W. T. Simpson, *J. Chem. Phys.*, **42**, 3175 (1965).
(32) D. T. Cromer and D. Liberman, *J. Chem. Phys.*, **53**, 1891 (1970).
(33) Supplementary material.
(34) W. C. Hamilton and J. A. Ibers, "Hydrogen Bonding in Solids", W. A. Benjamin, New York, N.Y., 1968.
(35) A. Bondi, *J. Phys. Chem.*, **68**, 441 (1964).
(36) A. Kobayashi, F. Marumo, and Y. Saito, *Acta Crystallogr., Sect. B*, **28**, 3591 (1972).
(37) A. Kobayashi, F. Marumo, and Y. Saito, *Acta Crystallogr., Sect. B*, **29**, 2443 (1973).
(38) M. R. Churchill, *Inorg. Chem.*, **12**, 1213 (1973).
(39) V. S. Yadara and V. M. Padmanabhan, *Acta Crystallogr., Sect. B*, **29**, 493 (1973).
(40) Y. Okaya N. R. Stemple, and M. I. Kay, *Acta Crystallogr.*, **21**, 237 (1966).
(41) G. K. Ambady and G. Kartha, *Acta Crystallogr., Sect. B*, **24**, 1540 (1968).
(42) J. E. Williams, P. J. Stang, and P. von R. Schleyer, *Annu. Rev. Phys. Chem.*, **19**, 531 (1968).
(43) E. J. Jacob, H. B. Thompson, and L. S. Bartell, *J. Chem. Phys.*, **47**, 3736 (1967).
(44) R. H. Boyd, *J. Chem. Phys.*, **49**, 2574 (1968).
(45) For bond torsion, rather than use a single contribution for a bond with the form $U_\phi = {}^1/_2A(1 + \cos 3\phi)$, where ϕ is the torsion angle, nine equal terms corresponding to each I–J–K–L combination about the I_3–J–K–L_3 bond were employed with a barrier constant of $A/9$. This overcomes two problems associated with an arbitrary choice of any I–J–K–L set to represent bond torsion: (1) the I or L atoms chosen may be involved in another strong (mainly nonbonded type) interaction giving a poor estimate of the torsion angle ϕ; (2) in molecules of high symmetry such as $[Co(tame)_2]^{3+}$ an arbitrary choice of a particular I–J–K–L set for different bonds around a symmetry axis passing through the K atom can lead to incorrect minimum energy configurations.
(46) M. R. Snow, *J. Am. Chem. Soc.*, **92**, 3610 (1970).
(47) R. J. Geue and M. R. Snow, *J. Chem. Soc. A*, 2981 (1971).
(48) R. L. Hilderbrant, *J. Chem. Phys.*, **51**, 1654 (1969).
(49) M. Dwyer, R. J. Geue, and M. R. Snow, *Inorg. Chem.*, **12**, 2057 (1973).
(50) B. Bosnich and J. M. Harrowfield, *J. Am. Chem. Soc.*, **94**, 3425 (1972).
(51) B. Bosnich and J. M. Harrowfield, *J. Am. Chem. Soc.*, **93**, 4086 (1971).
(52) S. F. Mason and B. J. Norman, *Chem. Commun.*, 335 (1965).
(53) B. Norden, *Acta Chem. Scand.*, **26**, 111 (1972).
(54) P. G. Beddoe, M. J. Harding, S. F. Mason, and B. J. Peart, *Chem. Commun.*, 1283 (1971).
(55) H. L. Smith and B. E. Douglas, *J. Am. Chem. Soc.*, **86**, 3885 (1964).
(56) S. F. Mason and B. J. Norman, *Proc. Chem. Soc., London*, 339 (1964).
(57) R. Larsson, S. F. Mason, and B. J. Norman, *J. Chem. Soc. A*, 301 (1966).
(58) S. F. Mason and B. J. Norman, *J. Chem. Soc. A*, 307 (1966).
(59) H. L. Smith and B. E. Douglas, *Inorg. Chem.*, **5**, 784 (1966).
(60) J. E. Sarneski and F. L. Urbach, *J. Am. Chem. Soc.*, **93**, 884 (1971).
(61) P. G. Beddoe and S. F Mason, *Inorg. Nucl. Chem. Lett.*, **4**, 433 (1968).
(62) J. R. Gollogly and C. J. Hawkins, *Chem. Commun.*, 689 (1968).
(63) A. M. Sargeson, *Transition Met. Chem.*, **3**, 303 (1966).
(64) K. R. Butler and M. R. Snow, *Inorg. Chem.*, **10**, 1838 (1971).
(65) A. J. McCaffery, S. F. Mason, and B. J. Norman, *Chem. Commun.*, 661 (1966).
(66) P. E. Schipper, *Inorg. Chim. Acta*, **12**, 199 (1975).
(67) E. G. Höhn and O. E. Weigang, *J. Chem. Phys.*, **48**, 1127 (1968).
(68) R. Ballard, A. McCaffery, and S. F. Mason, *Proc. Chem. Soc., London*, 331 (1962).
(69) E. Drouard and J. P. Mathieu, *C. R. Hebd. Seances Acad. Sci.*, **236**, 2395 (1953).
(70) K. R. Butler, Ph.D. Thesis, University of Adelaide, 1973.
(71) M. Iwata, K. Nakatsu, and Y. Saito, *Acta Crystallogr., Sect. B*, **25**, 2562 (1969).
(72) K. Nakatsu, *Bull. Chem. Soc. Jpn.*, **35**, 832 (1962).
(73) D. J. Hodgson, P. K. Hale, and W. E. Hatfield, *Inorg. Chem.*, **10**, 1061 (1971).
(74) E. N. Deusler and K. N. Raymond, *Inorg. Chem.*, **10**, 1486 (1971).
(75) J. H. Enemark, M. S. Quinby, L. L. Reed, M. J. Steuck, and K. K. Walthers, *Inorg. Chem.*, **9**, 2397 (1970).
(76) J. T. Veal and D. J. Hodgson, *Inorg. Chem.*, **11**, 597 (1972).
(77) D. Witiak, J. C. Clardy, and D. S. Martin, Jr., *Acta Crystallogr., Sect. B*, **28**, 2694 (1972).
(78) K. Nakatsu, Y. Saito, and H. Kuroya, *Bull. Chem. Soc. Jpn.*, **29**, 428 (1956).
(79) K. Nakatsu, M. Shiro, Y. Saito, and H. Kuroya, *Bull. Chem. Soc. Jpn.*, **30**, 158 (1957).
(80) S. F. Mason, *Q. Rev. Chem. Soc.*, **17**, 20 (1963).
(81) T. Bürer, *Helv. Chim. Acta*, **46**, 2388 (1963).
(82) A. J. McCaffery and S. F. Mason, *Mol. Phys.*, **6**, 359 (1963).
(83) M. Ito, F. Marumo, and Y. Saito, *Inorg. Nucl. Chem. Lett.*, **6**, 519 (1970).
(84) M. Ito, F. Marumo, and Y. Saito, *Acta Crystallogr., Sect. B*, **27**, 2187 (1971).
(85) S. Sato, Y. Saito, J. Fujita, and H. Ogino, *Inorg. Nucl. Chem. Lett.*, **10**, 669 (1974).